

Mono-, Bi-, and Trinuclear Metallacyclophanes Formed in Reactions between [Mo(NO){HB(3,5-Me₂C₃HN₂)₃}I₂] and Xylenedithiols. The X-ray Crystal Structures of [Mo(NO){HB(3,5-Me₂C₃HN₂)₃}{1,4-(SCH₂)₂C₆H₄}_n] (n = 2, 3)

Helen A. Hinton, Hongli Chen, Thomas A. Hamor, Christopher J. Jones,*
Ferida S. McQuillan, and Malcolm S. Tolley

School of Chemistry, The University of Birmingham, Edgbaston, Birmingham B15 2TT, U.K.

Received October 24, 1997

The reactions between [Mo(NO)(tp*)I₂] {tp* = HB(3,5-Me₂C₃HN₂)₃} and HE-EH {HE-EH = 1,3-(HSCH₂)₂C₆H₄ and 1,4-(HSCH₂)₂C₆H₄} afford the cyclic dimers [Mo(NO)(tp*)(E-E)]₂ and cyclic trimers [Mo(NO)(tp*)(E-E)]₃. These reactions also produce the monometallomacrocycles [Mo(NO)(tp*)(E-E)_x] (x = 2, 3) and, from 1,3-(SCH₂)₂C₆H₄, [Mo(NO)(tp*)(3-SCH₂C₆H₄CH₂)₂S]}. The reaction between [Mo(NO)(tp*)I₂] and 1,2-(HSCH₂)₂C₆H₄ affords, as its major product, the chelate complex [Mo(NO)(tp*)(1,2-(SCH₂)₂C₆H₄)], no metallomacrocycles being found among the reaction products in this case. Cyclic voltammograms of the macrocyclic complexes contain single reduction waves in the region -1.374 to -1.486 V (vs ferrocene/ferrocenium), and the binuclear metallomacrocycles show no electrochemically resolvable metal-metal interactions. The molecular structures of [Mo(NO){HB(3,5-Me₂C₃HN₂)₃}{1,4-(SCH₂)₂C₆H₄}_n] (n = 2, 3) have been determined crystallographically: [Mo(NO){HB(3,5-Me₂C₃HN₂)₃}{1,4-(SCH₂)₂C₆H₄}₂], C₃₁H₃₈BMoN₇OS₄, orthorhombic, space group *Pna*2₁, a = 16.193(8) Å, b = 12.878(5) Å, c = 16.620(5) Å, Z = 4; [Mo(NO){HB(3,5-Me₂C₃HN₂)₃}{1,4-(SCH₂)₂C₆H₄}₃], C₃₉H₄₆BMoN₇OS₆, monoclinic space group *P2*₁/*n*, a = 19.140(5) Å, b = 10.708(3) Å, c = 22.072(5) Å, β = 100.73(2)°, Z = 4.

Introduction

The synthesis of metallomacrocycles, in which metal centers together with ditopic ligands form a macrocyclic ring system, is a relatively recent development in macrocycle chemistry. An early example of such a system involved the linking of {M-(CO)₄} (M = Cr, Mo, W) centers by the ditopic ligand P(CH₂-OP)₃P to form tetranuclear metallomacrocycles.¹ Since then the use of equilibrium-controlled self-assembly reactions between polypyridyl ligands and metal centers such as Cu⁺, Pd²⁺, or Pt²⁺ has been an important source of new metallomacrocycles containing aryl rings.^{2–5} Other neutral ligands containing, for

example, pyrazolyl groups have also found use in this context.^{6–10} An alternative approach to metallomacrocyclic synthesis has involved the reaction of metal complexes containing suitably oriented substitution sites with anionic ditopic ligands. These reactions are not usually equilibrium controlled and so do not constitute self-assembly reactions in the strict sense. Examples of metallomacrocyclic hosts were obtained in this way from Cu²⁺ salts and proligands containing β-diketonate groups.¹¹ Subsequently the reaction between 1,3-(HOCH₂)₂C₆H₄ and [Zr(η⁵-C₅H₅)₂Me₂] was used to synthesize the cyclic dimer [{Zr(η⁵-C₅H₅)₂}{1,3-(O)₂C₆H₄}]₂.¹² In our laboratory we have used halide substitution by bifunctional proligands containing hydroxide, amide, or thiolate donor groups to synthesize a variety of metallomacrocycles containing octahedral metal centers derived from [M(NO)(tp*)I₂] (M = Mo, W) or [Mo(O)(tp*)Cl₂].¹³ The reactions between [Mo(NO)(tp*)I₂] and the “flexible” bridging ligands HE-EH {HE-EH = 1,3-(OCH₂)₂C₆H₄, 1,4-(OCH₂)₂C₆H₄ and 1,3-(OC₆H₄)₂CH₂} afford, as their major products, the syn and anti isomers of the cyclic dimers [Mo(NO)(tp*)(E-E)]₂, the isomer distribution depending on the nature of the bridging ligand E-E. The use of more “rigid” proligands, such as 1,3-(HO)₂C₆H₄, 1,4-(HO)₂C₆H₄, 2,7-

- (1) Stricklen, P. M.; Volcko, E. J.; Verkade, J. G. *J. Am. Chem. Soc.* **1983**, *105*, 2494–2945.
- (2) Lehn, J.-M. *Supramolecular Chemistry*; VCH Verlagsgesellschaft: Weinheim, 1995; pp 144–160.
- (3) (a) Fujita, M.; Yazaki, J. *J. Am. Chem. Soc.* **1990**, *112*, 5645–5646. (b) Fujita, M.; Nagao, S.; Iida, M.; Ogata, K.; Ogura, K. *J. Am. Chem. Soc.* **1993**, *115*, 1574–1576. (c) Fujita, M.; Ogura, K. *Coord. Chem. Rev.* **1996**, *148*, 249–264 and references therein. (d) Fujita, M.; Aoyagi, M.; Ogura, K. *Inorg. Chim. Acta* **1996**, *246*, 53–57. (e) Fujita, M.; Ibukuro, F.; Seki, H.; Osamu, K.; Imanari, M.; Ogura, K. *J. Am. Chem. Soc.* **1996**, *118*, 899–900.
- (4) (a) Stang, P. J.; Cao, D. H. *J. Am. Chem. Soc.* **1994**, *116*, 4981–4982. (b) Stang, P. J.; Whiteford, J. A. *Organometallics* **1994**, *13*, 3776–3777. (c) Stang, P. J.; Cao, D. H.; Saito, S.; Arif, A. M. *J. Am. Chem. Soc.* **1995**, *117*, 6273–6283. (d) Stang, P. J.; Chen, K. C.; Arif, A. M. *J. Am. Chem. Soc.* **1995**, *117*, 8793–8797. (e) Stang, P. J.; Olenyuk, B.; Arif, A. M. *Organometallics* **1995**, *14*, 5281–5289. (f) Stang, P. J.; Olenyuk, B. *Angew. Chem., Int. Ed. Engl.* **1996**, *35*, 732–736. (g) Whiteford, J. A.; Lu, C. V.; Stang, P. J. *J. Am. Chem. Soc.* **1997**, *118*, 2524–2533. (h) Stang, P. J.; Persky, N. E.; Manna, J. *J. Am. Chem. Soc.* **1997**, *118*, 4777–4778. (i) Stang, P. J.; Cao, D. H.; Chen, K.; Gray, G. M.; Muddiman, D. C.; Smith, R. D. *J. Am. Chem. Soc.* **1997**, *118*, 5163–5168. (j) Olenyuk, B.; Whiteford, J. A.; Stang, P. J. *J. Am. Chem. Soc.* **1996**, *118*, 8221–8230.
- (5) Ruttimann, S.; Bernardinalli, G.; Williams, A. F. *Angew. Chem., Int. Ed. Engl.* **1993**, *32*, 392–394.

- (6) Baker, A. T.; Crass, J. C.; Maniska, M.; Craig, D. C. *Inorg. Chim. Acta* **1995**, *230*, 225–229.
- (7) Bilyk, A.; Harding, M. M.; Turner, P.; Hambley, T. W. *J. Chem. Soc., Dalton Trans.* **1995**, 2549–2553.
- (8) Hartshorn, C. M.; Steel, P. J. *J. Chem. Soc., Chem. Commun.* **1997**, 541–542.
- (9) Chawla, S. K.; Gill, B. K. *Polyhedron* **1997**, *16*, 1315–1322.
- (10) Slone, R. V.; Yoon, D. I.; Calhounand, R. M.; Hupp, J. T. *J. Am. Chem. Soc.* **1995**, *117*, 11813–11814.
- (11) (a) Maverick, A. W.; Klavetter, F. E. *Inorg. Chem.* **1984**, *23*, 4130. (b) Maverick, A. W.; Buckingham, S. C.; Yao, Q.; Bradbury, J. R.; Stanley, G. G. *J. Am. Chem. Soc.* **1986**, *108*, 7430–7431.
- (12) Stephan, D. W. *Organometallics* **1990**, *9*, 2718–2723.

(HO)₂C₁₀H₆, and 4,4'-(HO)C₆H₄C₆H₄(OH), affords higher proportions of cyclic trimers and cyclic tetramers. In this paper we describe the reactions of [Mo(NO)(tp*)₂] with the xylenedithiols 1,*x*-(SCH₂)₂C₆H₄ (*x* = 2–4). In addition to the stereoselective formation of cyclic dimers, these reactions give rise to cyclic trimers and novel monometallic cyclophanes.

Experimental Section

General Details. All reactions were carried out under an atmosphere of dry nitrogen, but the reaction products were treated as air-stable. Dry, freshly distilled dichloromethane or toluene was used for all reactions. Triethylamine was dried over molecular sieves and stored over activated alumina. The compounds [Mo(NO)(tp*)₂]·C₆H₅CH₃ and [Mo(NO)(tp*)Cl₂] were prepared following known procedures.¹⁴ Column chromatography was carried out using silica gel 60 (70–230 mesh) supplied by Merck. TLC (thin-layer chromatography) was carried out on Merck aluminum sheets coated with silica gel 60 F₂₅₄ to a thickness of 0.2 mm.

Infrared spectra were recorded from KBr disks on a Perkin-Elmer 1600 series FT-IR spectrophotometer. UV/vis spectra were obtained using a Perkin-Elmer λ3 spectrophotometer. Solvent background corrections were made in all cases. Liquid secondary-ion mass spectra (LSIMS) were obtained from a VG Zabspec mass spectrometer utilizing a *m*-nitrobenzyl alcohol matrix and scanning in the positive ion mode at a speed of 5 s/decade, or in some cases electron impact mass spectrometry (EIMS). ¹H NMR spectra were recorded from solutions in CDCl₃ unless otherwise stated using a Bruker 300 MHz or Bruker AMX 400 instrument at room temperature unless otherwise stated. Cyclic voltammetry was carried out using an EG&G model 362 potentiostat and the Condecon 310 hardware/software package. Measurements were made using approximately 2 × 10⁻³ mol dm⁻³ solutions in dry dichloromethane under an atmosphere of nitrogen. A 0.2 mol dm⁻³ solution of [Bu₄N][BF₄] was used as the base electrolyte. A platinum bead electrode was used, and potentials were measured with reference to ferrocene added as an internal standard. The data obtained were reproducible, the experimental error being ±10 mV. Microanalyses were performed by the Microanalytical Laboratories of the University of Sheffield or the University of North London.

Preparation of [Mo(NO)(tp*){1,3-(SCH₂)₂C₆H₄}]₂, **1; [Mo(NO)(tp*){1,3-SCH₂C₆H₄CH₂S}]₂, **2**; [Mo(NO)(tp*){1,3-(SCH₂)₂C₆H₄}]₃, **3**; [Mo(NO)(tp*){1,3-(SCH₂)₂C₆H₄}]₂, **4**; and [Mo(NO)(tp*){1,3-(SCH₂)₂C₆H₄}]₃, **5**.**

A sample of [Mo(NO)(tp*)₂]·C₆H₅CH₃ (500 mg; 0.65 mmol) was dissolved in warm toluene (50 cm³) and an excess of triethylamine added (ca. 0.5 cm³). While this solution was being stirred, 1,3-(HSCH₂)₂C₆H₄ (110 mg; 0.65 mmol) was added and the mixture heated under reflux for 24 h. The resulting dark red/brown solution was allowed to cool and filtered to remove the precipitated [HNEt₃]⁺. The filtrate was evaporated to dryness, and the reaction products were separated by column chromatography using 60:40 hexane/dichloromethane as the eluant. Complex **1** was isolated from the first red/brown colored band (93 mg; 19%). ¹H NMR (400 MHz, C₂D₂Cl₄, 403 K): δ 7.21 [6H, m, overlapping signals, C₆H₄], 7.12 [2H, d, ³J_{HH} = 6 Hz, C₆H₄], 5.93, 5.79 [1H, s, 2H, s; C₃N₂HMe₂], 5.92 [2H, d, ²J_{HH} = 11 Hz, SCH₂(C₆H₄)], 5.79 [2H, s, C₃N₂HMe₂], 5.04 [2H, d, ²J_{HH} = 14 Hz, SCH₂(C₆H₄)], 3.62, 3.58 [2H, d, ²J_{HH} = 13 Hz; 2H, d, ²J_{HH} = 13 Hz, (C₆H₄)CH₂S], 2.54, 2.49, 2.38 [9H, s; 3H, s; 6H, s; C₃N₂H(CH₃)₂]. (+)-LSIMS: *m/z* 760 (M⁺), 666 (M - pz)⁺. Anal. Found: C, 49.3; H, 4.99; N, 12.2; S, 16.3. Calcd for C₃₁H₃₈BMoN₇OS₄: C, 49.0; H, 5.04; N, 12.9; S, 16.9. IR data (KBr disk): 2543 (ν_{BH}), 1653 (ν_{NO}) cm⁻¹.

Complex 2 was isolated as a bright red compound from the second band obtained from column chromatography (56 mg; 12%). ¹H NMR (400 MHz, CD₂Cl₂, 253 K): δ 7.31 [2H, t, ³J_{HH} = 8 Hz, C₆H₄], 7.27 [2H, t, ³J_{HH} = 7 Hz, C₆H₄], 7.18 [2H, d, ³J_{HH} = 8 Hz, C₆H₄], 6.91 [2H, s, C₆H₄], 6.30 [2H, d, ²J_{HH} = 13 Hz, SCH₂(C₆H₄)], 5.95, 5.82 [1H, s; 2H, s; C₃N₂HMe₂], 4.92 [2H, d, ²J_{HH} = 13 Hz, SCH₂(C₆H₄)], 3.34, 3.25 [2H, d, ²J_{HH} = 14 Hz; 2H, d, ²J_{HH} = 14 Hz, (C₆H₄)CH₂S], 2.49, 2.47, 2.44, 2.31 [3H, s; 6H, s; 3H, s; 6H, s, C₃N₂H(CH₃)₂]. Anal. Found: C, 51.2; H, 5.16; N, 13.4; S, 13.3. Calcd for C₃₁H₃₈BMoN₇OS₄: C, 51.2; H, 5.26; N, 13.5; S, 13.2%. (+)-LSIMS: *m/z* 728 (M⁺). IR data (KBr disk) 2545 (ν_{BH}), 1654 (ν_{NO}) cm⁻¹.

Complex 3 was isolated as a dark brown compound from the third band obtained from column chromatography (55 mg; 9%). ¹H NMR (300 MHz, CDCl₃, 293 K): δ 7.34–7.21 [3H, m, overlapping signals, C₆H₄], 7.20 [4H, d, ³J_{HH} = 7 Hz C₆H₄], 7.09 [1H, s, C₆H₄], 7.05 [2H, d, ³J_{HH} = 8 Hz, C₆H₄], 6.60 [2H, s, C₆H₄], 5.95, 5.75 [1H, s; 2H, s; C₃N₂HMe₂], 3.66 [4H, s br, (C₆H₄)CH₂S], 3.61 [4H, s br, (C₆H₄)CH₂S], 2.58, 2.47, 2.43, 2.34 [3H, s; 3H, s; 6H, s; 6H, s; C₃N₂H(CH₃)₂]. Anal. Found: C, 47.7; H, 4.81; N, 9.87; S, 21.0. Calcd for C₃₉H₄₆BMoN₇OS₆: C, 50.5; H, 5.00; N, 10.6; S, 20.7. (+)-LSIMS: *m/z* 928 (M⁺), 834 (M - pz)⁺, 760 (M - SC₆H₄S)⁺. IR data (KBr disk): 2549 (ν_{BH}), 1644 (ν_{NO}) cm⁻¹.

Complex 4 was isolated from the fourth brown/green band appearing on the chromatography column. This band consisted of a mixture of syn and anti isomers (total yield, 193 mg; 50%). (Anal. Found: C, 46.7; H, 5.00; N, 16.7; S, 11.1. Calcd for C₄₆H₆₀B₂Mo₂N₁₄O₂S₄: C, 46.7; H, 5.11; N, 16.6; S, 10.8.) The isomers **4a** and **4b** were separated using fractional crystallization from CH₂Cl₂/*n*-hexane mixtures. The less soluble isomer, **4a**, was obtained as a purple solid, which dissolved in CH₂Cl₂ to give a green colored solution. The second isomer, **4b**, remained in solution and was isolated as a dark brown solid after concentration of the solution by evaporation. Each isomer has been characterized individually although, in the absence of a crystal structure, it is not possible to determine unequivocally which is the syn and which the anti isomer.

Green/purple isomer, 4a: 112 mg; 29%. ¹H NMR (400 MHz, C₂D₂Cl₄, 413 K): δ 7.53, 7.04, 6.92 [2H, s; 2H, t; ³J_{HH} = 7 Hz; 4H, d, ³J_{HH} = 7 Hz, C₆H₄], 5.93, 5.74 [2H, s; 4H, s; C₃N₂HMe₂], 5.19, 4.92 [4H, d, ²J_{HH} = 12 Hz; 4H, d, ²J_{HH} = 13 Hz, SCH₂(C₆H₄)], 2.57, 2.47, 2.45, 2.34 [6H, s; 6H, s; 12H, s; 12H, s; C₃N₂H(CH₃)₂]. Anal. Found: C, 46.7; H, 5.01; N, 16.7; S, 11.1. Calcd for C₄₆H₆₀B₂Mo₂N₁₄O₂S₄: C, 46.7; H, 5.11; N, 16.6; S, 10.8. (+)-LSIMS: *m/z* 1183 (M⁺), 1015 (M - SC₆H₄S)⁺. IR data (KBr disk): 2546 (ν_{BH}), 1655 (ν_{NO}) cm⁻¹.

Brown isomer, 4b: 81 mg; 21%. ¹H NMR (400 MHz, C₂D₂Cl₄, 393 K): δ 6.69, 6.51 [2H, s, 6H, s; C₆H₄], 5.26, 5.14 [2H, s; 4H, s; C₃N₂HMe₂], 4.82, 4.52 [4H, d, ²J_{HH} = 12 Hz; 4H, d, ²J_{HH} = 14 Hz, (C₆H₄)CH₂S], 1.90, 1.86, 1.84, 1.72 [6H, s; 3H, s; 3H, s; 6H, s; C₃N₂H(CH₃)₂]. Anal. Found: C, 46.7; H, 5.21; N, 16.2; S, 11.0. Calcd for C₄₆H₆₀B₂Mo₂N₁₄O₂S₄: C, 46.7; H, 5.11; N, 16.6; S, 10.8. (+)-LSIMS: *m/z* 1183 (M⁺), 1015 (M - SC₆H₄S)⁺. IR data (KBr disk): 2547 (ν_{BH}), 1653 (ν_{NO}) cm⁻¹.

Complex 5 was isolated as a brown compound from the fifth band appearing on the chromatography column. This compound consists of a mixture of syn,syn and syn,anti isomers which could not be separated (total yield, 38 mg; 10%). ¹H NMR (300 MHz, CDCl₃, 293 K; assumed 3:1 syn,anti:syn,syn isomer mixture normalized to 1 trimer molecule): δ 7.3–6.9 [12H, br, overlapping signals C₆H₄], 5.96, 5.91, 5.88, 5.73, 5.72, 5.71 [³/₄H, s; 1¹/₂H, s; ³/₄H, s; 1¹/₂H, s; 3H, s; 1¹/₂H, s; C₃N₂HMe₂], 5.4–4.7 [very broad, overlapping signals, SCH₂(C₆H₄)], 2.68, 2.58, 2.50, 2.46, 2.44, 2.43, 2.40, 2.30 [2¹/₄H, s, 4¹/₂H, s; 2¹/₄H, s; 11¹/₄H, s; 4¹/₂H, s; 4¹/₂H, s; 9H, s; 15³/₄H, s; overlapping singlets, C₃N₂H(CH₃)₂]. Anal. Found: C, 46.6; H, 5.20; N, 16.6; S, 11.1. Calcd for C₆₉H₉₀B₃Mo₃N₂₁O₃S₆: C, 46.7; H, 5.11; N, 16.6; S, 10.8. (+)-LSIMS: *m/z* 1775 (M⁺). IR data (KBr disk): 2547 (ν_{BH}), 1654 (ν_{NO}) cm⁻¹.

Reaction of [Mo(NO)(tp*)Cl₂] with 1,3-(HSCH₂)₂C₆H₄. The preceding reaction was carried out following the same procedure and purification techniques but using [Mo(NO)(tp*)Cl₂] (321 mg; 0.65 mmol) in place of [Mo(NO)(tp*)₂]. Products **1–5** were separated as described above and were identified by spectroscopic and by TLC

- (13) (a) Jones, C. J.; McWhinnie, S. L. W.; McQuillan, F. S.; McCleverty, J. A. In *Molecular Electrochemistry of Inorganic, Bioinorganic and Organometallic Compounds*; Pombiero, A. J. L., McCleverty, J. A., Eds.; NATO ASI Series C; Kluwer Academic Publishers: Dordrecht, 1993, Vol. 385, p 89. (b) McQuillan, F. S.; Jones, C. J.; McCleverty, J. A. *Polyhedron* **1995**, *14*, 3157–3160. (c) McQuillan, F. S.; Jones, C. J. *Polyhedron* **1996**, *15*, 1553–1557. (d) McQuillan, F. S.; Chen, H.; Hamor, T. A.; Jones, C. J. *Polyhedron* **1996**, *15*, 3909–3913. (e) Berridge, T. E.; Jones, C. J. *Polyhedron* **1997**, *16*, 2329–2333.
- (14) Reynolds, S. J.; Smith, C. F.; Jones, C. J.; McCleverty, J. A.; Bower, D. C.; Templeton, J. L. *Inorg. Synth.* **1985**, *23*, 4–9.

Table 1. Yields of Metallomacrocycles Produced by Different Synthetic Routes

complex	synth meth and assoc yields (%)		
	1 step		2 step
	1:1 HE-EH + [Mo(NO) (tp*)I ₂]	1:1 HE-EH + [Mo(NO) (tp*)Cl ₂]	HE-EH + [{Mo(NO) (tp*)I ₂ (E-E)]
1^a	19	12	6
2^a	12	8	3
3^a	9	5	2
4^{a,b}	50	58	77
ratio 4a:4b^c	42:58	40:60	45:55
5^{a,b}	10	12	10
7^d	10		6
8^d	6		2
9^{b,d}	33		35
ratio 9a:9b^{c,d}	45:55		45:55
10^{b,d}	40		37

^a HE-EH = 1,3-(HSCH₂)₂C₆H₄. ^b Total yield of isomer mixture. ^c Ratio expressed as percentage of each isomer, total 100%. ^d HE-EH = 1,4-(HSCH₂)₂C₆H₄.

measurements. The yields of each complex which were obtained in this way are reported in Table 1.

{[Mo(NO)(tp*)I₂]{1,3-(SCH₂)₂C₆H₄}]₂, **6**. A sample of [Mo(NO)(tp*)I₂]-C₆H₅CH₃ (1.5 g; 1.95 mmol) was dissolved in warm toluene (80 cm³) with stirring and 1,3-(HSCH₂)₂C₆H₄ (110 mg; 0.65 mmol) added before the mixture was heated under reflux for 48 h. The resulting dark brown solution was allowed to cool and filtered. The filtrate was evaporated to dryness and purified using column chromatography with 60:40 hexane/dichloromethane as the eluant. The major brown band was collected to give **6** as an orange/brown solid (252 mg; 31%). ¹H NMR (293 K, CDCl₃, 300 MHz): δ 7.49, 7.36–7.19 [1H, s; 4H, m; overlapping signals, C₆H₄], 5.96, 5.82, 5.78 [2H, s; 2H, s; 2H, s; C₃N₂HMe₂], 3.73 [4H, d, ²J_{HH} = 11 Hz, SCH₂(C₆H₄)CH₂S], 2.57, 2.49, 2.37, 2.35, 2.21 [6H, s; 12H, s; 6H, s; 6H, s; 6H, s; C₃N₂H(CH₃)₂]. Anal. Found: C, 36.0; H, 4.09; N, 15.5; S, 4.9. Calcd for C₃₈H₅₂B₂I₂Mo₂N₁₄O₂S₂: C, 36.0; H, 4.13; N, 15.5; S, 5.1. (+)-LSIMS: *m/z* 1268 (M⁺), 1141 (M – I)⁺. IR data (KBr disk): 2550 (ν_{BH}), 1674 (ν_{NO}) cm⁻¹.

Reaction of {[Mo(NO)(tp*)I₂]{1,3-(SCH₂)₂C₆H₄}] with 1,3-(HSCH₂)₂C₆H₄. A sample of **6** (200 mg; 0.158 mmol) was dissolved in warm toluene (50 mL) and an excess of triethylamine (ca. 0.5 cm³) was added. While this solution was being stirred, 1,3-(HSCH₂)₂C₆H₄ (27 mg; 0.158 mmol) was added and the mixture heated under reflux for 24 h. The resulting dark red/brown solution was allowed to cool and filtered and the filtrate evaporated to dryness. The products **1–5** were separated as described above for the reaction between [Mo(NO)(tp*)I₂] and 1,3-(HSCH₂)₂C₆H₄. The products were identified spectroscopically and by TLC. Yields of each complex are reported in Table 1.

Preparation of [Mo(NO)(tp*){1,4-(SCH₂)₂C₆H₄}]₂, **7; [Mo(NO)(tp*){1,4-(SCH₂)₂C₆H₄}]₃, **8**; [Mo(NO)(tp*){1,4-(SCH₂)₂C₆H₄}]₂, **9**; and [Mo(NO)(tp*){1,4-(SCH₂)₂C₆H₄}]₃, **10**.** Complexes **7–10** were synthesized according to the procedure described for **1–5** above using [Mo(NO)(tp*)I₂]-C₆H₅CH₃ (300 mg; 0.39 mmol) and 1,4-(HSCH₂)₂C₆H₄ (66 mg; 0.39 mmol).

Complex 7 was isolated from the first red band to elute from the column (30 mg; 10%). ¹H NMR (300 MHz, CDCl₃, 293 K): δ 7.05 [4H, s, br, C₆H₄], 6.78 [4H, d, ³J_{HH} = 8 Hz, C₆H₄], 6.32 [2H, d, ²J_{HH} = 13 Hz, SCH₂(C₆H₄)], 5.97, 5.77 [1H, s; 2H, s; C₃N₂HMe₂], 4.95 [2H, d, ²J_{HH} = 13 Hz, SCH₂(C₆H₄)], 3.89, 3.45 [2H, d, ²J_{HH} = 14 Hz; 2H, d, ²J_{HH} = 15 Hz, (C₆H₄)CH₂S], 2.71, 2.52, 2.48, 2.38 [3H, s; 6H, s; 3H, s; 6H, s; C₃N₂H(CH₃)₂]. Anal. Found: C, 49.2; H, 4.94; N, 12.9; S, 17.0. Calcd for C₂₈H₃₈BMoN₇O₅S₄: C, 49.0; H, 5.04; N, 12.9; S, 16.9. (+)-LSIMS: *m/z* 760 (M⁺). IR data (KBr disk): 2544 (ν_{BH}), 1649 (ν_{NO}) cm⁻¹. Crystals suitable for X-ray analysis were obtained from CH₂Cl₂/hexane solutions.

Complex 8 was isolated from the second brown band eluted from the chromatography column (20 mg; 6%). ¹H NMR (400 MHz, C₂D₂-Cl₄, 403 K): δ 7.19, 7.18, 7.06 [4H, d, ³J_{HH} = 8 Hz; 4H, s; 4H, d, ³J_{HH}

= 6 Hz, C₆H₄], 5.93, 5.77 [1H, s; 2H, s; C₃N₂HMe₂], 5.39, 5.02 [2H, d, ²J_{HH} = 14 Hz; 2H, d, ²J_{HH} = 14 Hz, SCH₂(C₆H₄)], 3.69 [4H, s; 4H, s; (C₆H₄)CH₂S], 2.55, 2.49, 2.35 [3H, s; 9H, s; 6H, s; C₃N₂H(CH₃)₂]. Anal. Found: C, 53.6; H, 4.90; N, 8.83; S, 20.1. Calcd for C₃₉H₄₆BMoN₇O₅S₆: C, 50.5; H, 5.00; N, 10.6; S, 20.7. (+)-LSIMS: *m/z* 928 (M⁺), 834 (M – pz)⁺. IR data (KBr disk): 2547 (ν_{BH}), 1652 (ν_{NO}) cm⁻¹. Crystals suitable for X-ray analysis were obtained from CH₂Cl₂/hexane solutions.

Complex 9 was isolated from the third brown/red band to elute from the chromatography column. This compound consisted of a mixture of syn and anti isomers (total 75 mg; 33%). (Anal. Found: C, 46.7; H, 5.0; N, 16.7; S, 11.1. Calcd for C₄₆H₆₀B₂Mo₂N₁₄O₂S₄: C, 46.7; H, 5.11; N, 16.6; S, 10.8.) The isomers could be separated by repeated column chromatography using 70:30 hexane/dichloromethane as the eluant. A red isomer, **9a**, was eluted first followed by a brown isomer, **9b**. Each isomer has been characterized individually although it is not possible to determine unequivocally which is the syn and which the anti isomer in the absence of a crystal structure.

Red isomer, 9a: 41 mg; 55%. ¹H NMR (400 MHz, C₂D₂Cl₄, 403 K): δ 7.07 [8H, s, C₆H₄], 5.93, 5.72 [2H, s; 4H, s; C₃N₂HMe₂], 5.51, 4.95 [4H, d, ²J_{HH} = 14 Hz; 4H, d, ²J_{HH} = 14 Hz, SCH₂(C₆H₄)], 2.67, 2.46, 2.32 [6H, s; 18H, s; 12H, s; C₃N₂H(CH₃)₂]. Anal. Found: C, 46.9; H, 5.03; N, 16.7; S, 11.0. Calcd for C₄₆H₆₀B₂Mo₂N₁₄O₂S₄: C, 46.7; H, 5.11; N, 16.6; S, 10.8. (+)-LSIMS: *m/z* 1183 (M⁺), 1088 (M – pz)⁺. IR data (KBr disk) 2549 (ν_{BH}), 1656 (ν_{NO}) cm⁻¹.

Brown isomer, 9b: 34 mg; 45%. ¹H NMR (300 MHz, CDCl₃, 293 K): δ 7.26–7.12 [8H, m, overlapping signals, C₆H₄], 5.92, 5.75, 5.72 [1H, s; 1H, s; 1H, s, C₃N₂HMe₂], 5.16 [4H, s, broad signal, SCH₂(C₆H₄)], 3.51, 3.40 [2H, d, ²J_{HH} = 11 Hz; 2H, d, ²J_{HH} = 12 Hz, (C₆H₄)CH₂S], 2.61, 2.54, 2.47, 2.45, 2.41, 2.39, 2.32 [36H, overlapping signals, C₃N₂H(CH₃)₂]. Anal. Found: C, 46.5; H, 5.24; N, 16.5; S, 11.2. Calcd for C₄₆H₆₀B₂Mo₂N₁₄O₂S₄: C, 46.7; H, 5.11; N, 16.6; S, 10.8. (+)-LSIMS: *m/z* 1183 (M⁺), 1088 (M – pz)⁺. IR data (KBr disk): ν_{max} 2544 (ν_{BH}), 1654 (ν_{NO}) cm⁻¹.

Complex 10 was isolated from the fourth brown band to elute from the chromatography column. This compound consisted of a mixture of isomers which could not be separated (total, 92 mg; 40%). ¹H NMR (300 MHz, CDCl₃, 293 K, assumed 3:1 syn:anti:anti:anti isomer mixture normalized to 1 trimer molecule): δ 7.3–7.0 [12H, br, overlapping signals C₆H₄], 5.94, 5.92, 5.91, 5.77, 5.72 [³/₄H, s; 1¹/₂H, s; 1¹/₂H, s; 3¹/₄H, s; 4¹/₂H, s; C₃N₂HMe₂], 5.6–4.5 [6H very broad, overlapping signals, SCH₂(C₆H₄)], 3.7–3.3 [6H very broad, overlapping signals, SCH₂(C₆H₄)], 2.60, 2.46, 2.45, 2.43, 2.42, 2.39, 2.32 [4¹/₂H, s; 4¹/₂H, overlapping signals; 9H, s; 4¹/₂H, s; 9H, s; 4¹/₂H, s; 18H, s; C₃N₂H(CH₃)₂]. Anal. Found: C, 46.9; H, 5.20; N, 16.5; S, 11.2. Calcd for C₆₉H₉₀B₃Mo₃N₂₁O₃S₆: C, 46.7; H, 5.11; N, 16.6; S, 10.8. (+)-LSIMS: *m/z* 1775 (M⁺). IR data (KBr disk): 2544 (ν_{BH}), 1652 (ν_{NO}) cm⁻¹.

{[Mo(NO)(tp*)I₂]{1,4-(SCH₂)₂C₆H₄}]₂, **11**. A sample of [Mo(NO)(tp*)I₂]-C₆H₅CH₃ (1.5 g; 1.95 mmol) was dissolved in warm toluene (80 cm³) with stirring, 1,4-(HSCH₂)₂C₆H₄ (110 mg; 0.65 mmol) was then added and the mixture heated under reflux for 48 h. The resulting dark brown colored solution was allowed to cool and then filtered. The filtrate was evaporated to dryness and purified using column chromatography with 60:40 hexane/dichloromethane as the eluant. The major orange band was collected and afforded the complex **11** as an orange/brown solid (238 mg; 20%). ¹H NMR (300 MHz, CDCl₃, 293 K): δ 7.45 [4H, s, C₆H₄], 5.96, 5.82, 5.77 [2H, s; 2H, s; 2H, s; C₃N₂HMe₂], 3.75–3.52 [4H, m, overlapping signals, SCH₂(C₆H₄)CH₂S], 2.57, 2.48, 2.36, 2.34, 2.18 [6H, s; 12H, s; 6H, s; 6H, s; 6H, s; C₃N₂H(CH₃)₂]. Anal. Found: C, 36.1; H, 4.19; N, 15.3; S, 5.0. Calcd for C₃₈H₅₂B₂I₂Mo₂N₁₄O₂S₂: C, 36.0; H, 4.13; N, 15.5; S, 5.1%. (+)-LSIMS: *m/z* 1269 (M⁺), 1141 (M – I)⁺. IR data (KBr disk): 2550 (ν_{BH}), 1676 (ν_{NO}) cm⁻¹.

Reaction of {[Mo(NO)(tp*)I₂]{1,4-(SCH₂)₂C₆H₄}] with 1,4-(HSCH₂)₂C₆H₄. A sample of **11** (175 mg; 0.14 mmol) was dissolved in warm toluene (50 cm³), an excess of triethylamine (ca. 0.5 mL) was added with stirring followed by 1,4-(HSCH₂)₂C₆H₄ (24 mg; 0.14 mmol), and the solution was heated under reflux for 24 h. The resulting dark red/brown colored solution was allowed to cool and filtered to remove precipitated triethylammonium salt. The filtrate was evaporated to

Table 2. Crystallographic Data

	7	8
empirical formula	C ₃₁ H ₃₈ BN ₇ OS ₄ Mo	C ₃₉ H ₄₆ BN ₇ OS ₆ Mo
fw	759.7	927.9
cryst syst	orthorhombic	monoclinic
space group	<i>Pna</i> 2 ₁ / <i>n</i>	<i>P</i> 2 ₁ / <i>n</i>
<i>a</i> , Å	16.193(8)	19.140(5)
<i>b</i> , Å	12.878(5)	10.708(3)
<i>c</i> , Å	16.620(5)	22.072(5)
β , deg		100.73(2)
<i>V</i> , Å ³	3466(2)	4445(2)
<i>Z</i>	4	4
<i>D</i> _c	1.456	1.387
μ (Mo K α), mm ⁻¹	0.656	0.616
cryst size, mm	0.2 × 0.15 × 0.15	0.3 × 0.25 × 0.2
θ range, deg	2.0–25.3	1.3–25.2
reflns collected		
[<i>I</i> > σ (<i>I</i>)]	13 593	18 972
unique reflns	5013	6851
<i>R</i> _{int}	0.0588	0.0551
variables	406	496
Δ/σ (max)	0.002	0.002
$\Delta\rho$, e Å ⁻³	0.32, -0.91	0.44, -0.49
<i>R</i> ₁ , w <i>R</i> ₂ ^a	0.1133, 0.1561	0.0906, 0.1169
obsd reflns [<i>I</i> > 2 σ (<i>I</i>)]	3626	5446
<i>R</i> ₁ , w <i>R</i> ₂ ^a obsd		
reflns	0.0646, 0.1286	0.0550, 0.0976
<i>w</i> (<i>a</i> , <i>b</i>) ^b	0.071, 0	0.033, 0.97

^a w*R*₂ = $[\sum w(F_o^2 - F_c^2)^2 / \sum w(F_o^2)^2]^{1/2}$. ^b *w* = $1/[\sigma^2(F_o^2) + (aP)^2 + bP]$ where $P = (F_o^2 + 2F_c^2)/3$.

dryness and contained products **7–10**, which were separated by column chromatography as described above for the reaction between [Mo(NO)(tp*)I₂] and 1,4-(HSCH₂)₂C₆H₄ and identified by spectroscopic and TLC measurements. The yields of each complex which were obtained in this way are reported in Table 1.

[{Mo(NO)(tp*)}{1,2-(SCH₂)₂C₆H₄}]₂, **12**. Complex **12** was synthesized and purified by the method described for **1** using [Mo(NO)(tp*)I₂]-C₆H₅CH₃ (500 mg; 0.65 mmol) with *o*-xylenedithiol, 1,2-(HSCH₂)₂C₆H₄ (110 mg; 0.65 mmol). The first orange colored band was collected to afford the chelate complex (199 mg; 55%). ¹H NMR (300 MHz, CDCl₃, 293 K): δ 7.21 [4H, d, ³*J*_{HH} = 3 Hz, C₆H₄], 6.17 [2H, d, ²*J*_{HH} = 14 Hz, SCH₂C₆H₄], 5.82, 5.73 [1H, s; 2H, s; C₃N₂HMe₂], 5.25 [2H, d, ²*J*_{HH} = 14 Hz, C₆H₄CH₂S], 2.43, 2.39, 2.38 [3H, s; 9H, s; 6H, s; C₃N₂H(CH₃)₂]. Anal. Found: C, 47.0; H, 5.15; N, 16.6; S, 11.0. Calcd for C₂₃H₃₀N₇OS₂BMo: C, 46.7; H, 5.11; N, 16.6; S, 10.8. (+)-LSIMS: *m/z* 592 (M⁺). IR data (KBr disk): 2543 (ν_{BH}), 1628 (ν_{NO}) cm⁻¹.

Structural Studies. X-ray data for the complexes **7** and **8** were collected on a Rigaku R-axis II area-detector diffractometer at 293(2) K using graphite-monochromated Mo K α radiation. The structures were determined by direct methods¹⁵ and refined¹⁶ on *F*² by full-matrix least squares with anisotropic displacement parameters for the non-hydrogen atoms. Hydrogen atoms were placed in calculated positions with isotropic displacement parameters. Crystallographic and refinement data are listed in Table 2. Figures depicting the structures were prepared using ORTEP,¹⁷ the thermal ellipsoids being drawn at the 30% probability level.

Results and Discussion

Synthetic Studies. Two approaches to the syntheses of the metallocyclophanes were employed. The first and simplest

approach merely involved a single-step reaction between [Mo(NO)(tp*)I₂] and 1,*x*-(HSCH₂)₂C₆H₄ (*x* = 3, 4) in a 1:1 molar ratio. Triethylamine was added to the reaction mixture as this reagent has been found to facilitate the substitution of both iodide ligands in [Mo(NO)(tp*)I₂] and consumes the HI liberated during the reaction.¹⁸ The second approach involved two steps. The bimetallic complexes [{Mo(NO)(tp*)I₂}]₂{1,*x*-(SCH₂)₂C₆H₄}] were synthesized in the first step¹⁹ and then treated with a second equivalent of the bridging proligand in a second reaction step. Although TLC (thin-layer chromatography) indicated that metallomacrocyclic products had begun to appear after only 10 min, the reaction mixtures were heated under reflux overnight in toluene to drive them to completion. Reactions involving [Mo(NO)(tp*)Cl₂] and [Mo(NO)(tp*)(OMe)₂] in place of [Mo(NO)(tp*)I₂] were also carried out to assess the effect of changing the reactivity and redox potential of the precursor metal complex. Finally the reaction between [Mo(NO)(tp*)I₂] and the potentially chelating proligand 1,2-(HSCH₂)₂C₆H₄ was also investigated to more fully assess how the pattern of substitution on the aryl ring affects the metallomacrocyclic formation reaction.

The complexes **1–5** (Figure 1) were formed in the reactions between 1,3-xylenedithiol and the dihalide complexes [Mo(NO)(tp*)(X)₂] (X = Cl, I) or the bimetallic complex [{Mo(NO)(tp*)I₂}]₂{1,3-(SCH₂)₂C₆H₄}], **6**. In addition to the cyclic oligomers **4** and **5**, which were expected to form, three unexpected products, **1–3**, were also isolated (Figure 1). The infrared spectra of all five compounds contained bands attributable to ν_{BH} at ca. 2550 and ν_{NO} at ca. 1650 cm⁻¹ in accord with the presence of the {Mo(NO)(tp*)} moiety. The ¹H NMR spectra of **1**, **2**, and **3** contained signals of relative areas 2:1 in the region δ 5.7–6.0 and 6:6:3:3 in the region 2.3–2.6 ppm attributable to the tp* ligand. This pattern is consistent with structures in which the tp* ligand is bisected by a plane of symmetry, on the NMR time scale at least. The relative areas of the signals due to the tp* ligand protons in the spectra of **1**, **2**, and **3**, and those of the aryl ligands, are consistent with respective tp*:{-(CH₂)₂C₆H₄-} ratios of 1:2, 1:2, and 1:3. At room temperature the methylene proton signals of these compounds are broadened by dynamic processes. The accessible temperature range was too limited to allow meaningful measurements of the energy barriers involved, but limiting spectra of **1** could be obtained at 403 K and of **2** at 253 K. To obtain information about the degree of oligomerization, if any, in these compounds, the LSIMS spectra of **1**, **2**, and **3** were recorded and found to contain respective molecular ions at *m/z* 760, 728, and 928. These values are consistent with the formulation of **1**, **2**, and **3** as the monometallic cycles [Mo(NO)(tp*){1,3-(SCH₂)₂C₆H₄}]₂, **1**, [Mo(NO)(tp*)(1,3-SCH₂C₆H₄-CH₂)₂S], **2**, and [{Mo(NO)(tp*)}{1,3-(SCH₂)₂C₆H₄}]₃, **3**, which contain oligomerized dithiol ligands linked by disulfide or, in the case of **2**, thioether groups. The elemental analyses of **1** and **2** were consistent with their formulations, but analyses of **3** showed a low carbon value, although values for H, N, and S were within 0.7% of the expected figure, suggesting that the sample was not completely pure.

The unexpected products **1–3** were formed in significant yields, which varied according to the preparative method used (Table 1). The single-step procedure produced yields in the

(15) Molecular Structure Corporation, TeXsan. Single-Crystal Structure Analysis Software, version 1.6. (1993), MSC, 3200 Research Forest Drive, TX 77381.

(16) Sheldrick, G. M. *SHELXL-93, Program for Crystal Structure Refinement*; University of Göttingen: Göttingen, 1993.

(17) Johnson, C. K. ORTEP. Report ORNL-5138; Oak Ridge National Laboratory: Oak Ridge, TN, 1976.

(18) McCleverty, J. A. *Chem. Soc. Rev.* **1983**, *12*, 331–360.

(19) (a) Charsley, S. M.; Jones, C. J.; McCleverty, J. A.; Neaves, B. D.; Reynolds, S. J. *Trans. Met. Chem.* **1986**, *11*, 329–334. (b) McCleverty, J. A.; Rae, A. E.; Wolochowicz, I.; Bailey, N. A.; Smith, J. M. A. J. *Chem. Soc., Dalton Trans.* **1982**, 429–438.

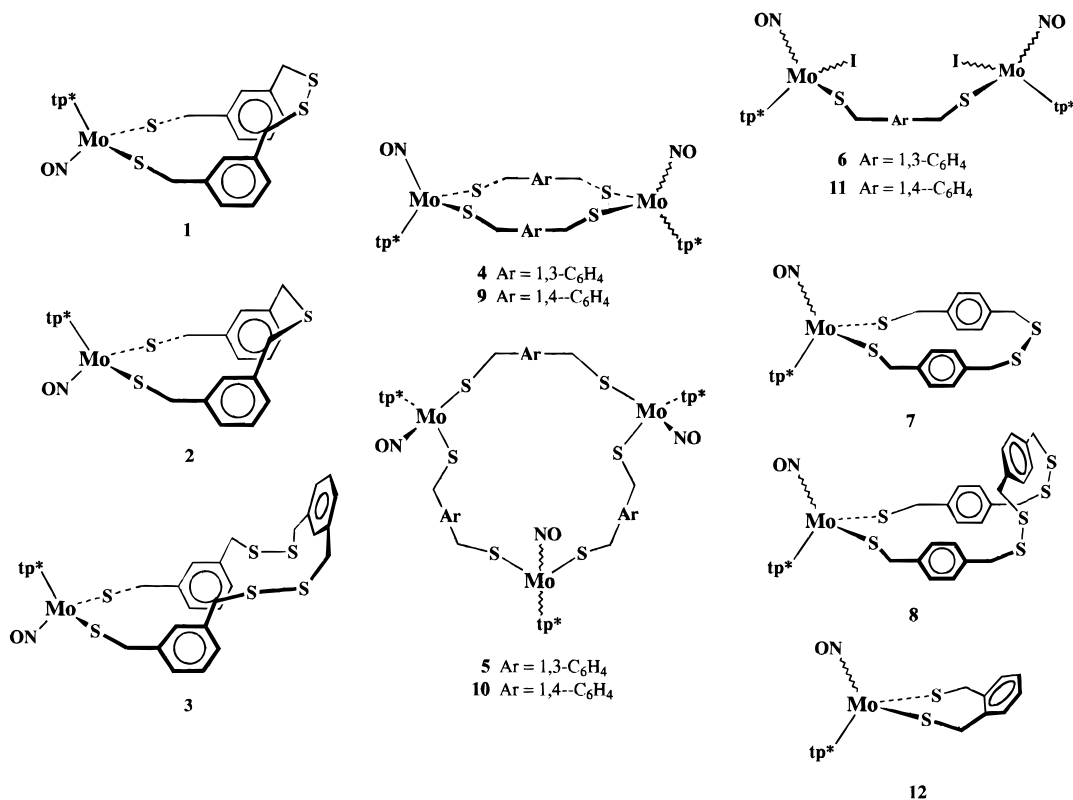


Figure 1. Structural formulas for compounds 1–12.

range 5–19% whereas the second step of the two-step procedure, utilizing $[\{\text{Mo}(\text{NO})(\text{tp}^*)\text{I}\}_2\{1,3-(\text{SCH}_2)_2\text{C}_6\text{H}_4\}]$, **6**, as an intermediate produced substantially lower yields, in the range 2–6%. Gas chromatography–mass spectroscopy studies provided no evidence for the presence of significant amounts of disulfides or other oxidized byproducts in the xylenedithiol used as a reagent, and the ¹H NMR spectrum contained no detectable signals which might be attributed to oxidized impurities. Since compounds **1–3** could not be detected in samples of **4** or **5** which had been stirred in air in a slurry of silica gel in dichloromethane and hexane (60:40 v/v mixture) for several days, they do not appear to be formed from the cyclic oligomers **4** and **5** during the purification of the reaction mixture. Thus the thiol ligand oligomers appear to be formed during the reaction with $[\text{Mo}(\text{NO})(\text{tp}^*)(\text{X})_2]$ or **6**.

The mechanism of formation of the monometallic macrocyclic complexes remains uncertain. They seem to form most readily during the reaction with $[\text{Mo}(\text{NO})(\text{tp}^*)\text{I}_2]$ and least readily in the reaction with **6**. One possible explanation is that $[\text{Mo}(\text{NO})(\text{tp}^*)(\text{X})_2]$ acts as an oxidant, forming disulfides in situ. These disulfides could then react with further $[\text{Mo}(\text{NO})(\text{tp}^*)(\text{X})_2]$ to produce the monometallic cycles. It is well established that the dihalide complexes $[\text{Mo}(\text{NO})(\text{tp}^*)(\text{X})_2]$ undergo facile reductions²⁰ to the 17-electron complexes $[\text{Mo}(\text{NO})(\text{tp}^*)(\text{X})_2]^-$ and, in the case of $[\text{Mo}(\text{NO})(\text{tp}^*)(\text{Cl})_2]$, this has been effected by reaction with a thioether.^{20b} The respective reduction potentials of $[\text{Mo}(\text{NO})(\text{tp}^*)\text{I}_2]$, $[\text{Mo}(\text{NO})(\text{tp}^*)(\text{Cl})_2]$, and $[\{\text{Mo}(\text{NO})(\text{tp}^*)\text{I}\}_2\{1,3-(\text{SCH}_2)_2\text{C}_6\text{H}_4\}]$ are 0.22, –0.09, and –0.38 V²⁰ (vs SCE), and in a qualitative way, the trends in the yields of **1–3** do follow this trend in reduction potentials. However, we have

no direct evidence that simple redox chemistry is involved in the formation of **1** and **3**, rather than some other chemical process, and the formation of **2** cannot easily be rationalized in terms of simple redox processes. Unsurprisingly mass spectrometric (EIMS) studies of the products from the reaction of xylenedithiol with tetrabutylammonium iodide showed no evidence of disulfide formation. However, the EIMS of the product of a reaction with NEt₃ contained an ion at *m/z* 304 having an intensity of 67% compared to that of the molecular ion at *m/z* 170. This could be attributable to the formation of the macrocycle $(\text{SCH}_2\text{C}_6\text{H}_4\text{CH}_2)_2\text{S}$ and suggests that the presence of NEt₃ in the reaction mixture may account for the formation of **2**.

The major product of the reaction between $[\text{Mo}(\text{NO})(\text{tp}^*)(\text{X})_2]$ and 1,3-(HSCH₂)₂C₆H₄ is the cyclic dimer $[\text{Mo}(\text{NO})(\text{tp}^*)(\text{SCH}_2\text{C}_6\text{H}_4\text{CH}_2\text{S})_2]$, **4**. A slightly higher yield is obtained when X = Cl (58%) than when X = I (50%). However, an even higher yield (77%) is obtained from the reaction involving $[\{\text{Mo}(\text{NO})(\text{tp}^*)\text{I}\}_2\{1,3-(\text{SCH}_2)_2\text{C}_6\text{H}_4\}]$, although the overall yield for this two-step route is only 24%, offering a significant disadvantage over the single-step procedure. This cyclic dimer may exist as syn and anti isomers depending upon the relative orientation of the two nitrosyl ligands in the complex. The different solubilities of the two isomers in dichloromethane/hexane mixtures provided a means of separation since one isomer, **4a**, which is green in solution, readily precipitates as a bright purple solid. The second isomer, **4b**, which is brown in color, remains in solution. The isomers **4a** and **4b** were isolated in similar relative proportions no matter which synthetic route was used. The two isomers give molecular ions at *m/z* = 1183 in their LSIMS spectra, in accord with their formulation as cyclic dimers, but exhibit different ¹H NMR spectra. In both cases the pattern of signals is in accord with the presence of a plane of symmetry bisecting the tp* ligands and the relative areas of the signals due to the tp* and xylyl protons are consistent with

(20) (a) Briggs, T. N.; Colquhoun, H.; El Murr, N.; Jones, C. J.; McCleverty, J. A.; Neaves, B. D.; Adams, H.; Bailey, N. A. *J. Chem. Soc., Dalton Trans.* **1985**, 1249–1254. (b) McWhinnie, S. L. W.; Jones, C. J.; McCleverty, J. A.; Collison, D.; Mabbs, F. E. *Polyhedron* **1992**, *11*, 2639–2643.

a tp*: $-\text{CH}_2\text{C}_6\text{H}_4\text{CH}_2-$ ratio of 1:1. Once again the methylene proton signals of **4a** and **4b** are broadened by dynamic processes. Limiting spectra were obtained at 400 MHz on heating the solutions, but on cooling, the spectrum of **4a** became very complex, indicating the presence of several conformers. The ^1H NMR spectra do not provide a sound basis for determining which is the syn and which the anti isomer, but the isomeric structures may be very tentatively assigned on the basis of solubilities since it has been generally found that the anti isomers of bimetallomacrocycles containing the $\{\text{Mo}(\text{NO})(\text{tp}^*)\}$ moiety are less soluble than the syn isomers.²¹ If this generalization extends to these thiolate complexes, then **4a** would have the anti structure and **4b** the syn. The isomer distribution for each reaction method was determined by ^1H NMR spectroscopy through comparing the integrations of the tp* protons for each isomer in the crude isomer mixture obtained from the chromatography column. The brown isomer, **4b**, was obtained in slightly lower proportions (40–45%) than the green/purple isomer, **4a** (55–60%), but the reactions are poorly selective in this respect.

The cyclic trimer, **5**, is also produced in the reaction, again in similar relative proportions (10–12%) no matter which synthetic route is used. The LSIMS spectrum of this complex contained a molecular ion at $m/z = 1775$ in accord with its formulation as a cyclic trimer and contained no significant ion intensity at $m/z = 1183$ which might have been attributed to the presence of some cyclic dimer. This complex can exist as syn,syn- or syn,anti isomers depending upon the relative orientations of the three nitrosyl ligands. These isomers could not be separated by column chromatography or fractional crystallization, but on purely statistical grounds, it might be expected that the ratio of syn,syn to syn,anti isomers formed would be 1:3. The syn,syn isomer should exhibit a fairly simple ^1H NMR spectrum since each $\{\text{Mo}(\text{NO})(\text{tp}^*)\}$ unit is equivalent and is bisected by a plane of symmetry. The pyrazolyl C⁴ protons should give rise to two singlets in the area ratio 6:3, and the pyrazolyl methyl protons should give rise to four signals in the area ratio 18:18:9:9. In the syn,anti isomer only one of the three $\{\text{Mo}(\text{NO})(\text{tp}^*)\}$ units is bisected by a plane of symmetry, the remaining two units being related by that plane (Figure 2). This gives rise to five environments for the nine pyrazolyl C⁴ protons with an occupancy ratio of 2:2:2:2:1. The pyrazolyl methyl protons are expected to be in 10 different environments with a proton occupancy ratio of 6:6:6:6:6:6:6:6:3:3. However, signal overlap is likely to reduce the total number of signals observed, especially in the spectrum of an isomer mixture. Assuming a 1:3 ratio of syn,syn: syn,anti isomers, the ^1H NMR spectrum of the isomer mixture will comprise a one-third contribution from the syn,syn isomer and a full contribution from the syn,anti isomer leading to seven signals from the pyrazolyl C⁴ protons in the area ratios 2:2:2:2:2:1:1 and 14 signals from the pyrazolyl methyl protons in the area ratios 6:6:6:6:6:6:6:6:3:3:3:3. These values correspond to four $\{\text{Mo}(\text{NO})(\text{tp}^*)\}$ units and must be multiplied by $3/4$ to normalize them to a single trimer molecule. The ^1H NMR spectrum of **5** shows evidence for dynamic processes which broaden the aryl and methylene proton signals, but a fairly well resolved spectrum of the tp* protons was obtained at 293 K. The relative areas of the pyrazolyl C⁴ proton signals were found to be $3/4:1\frac{1}{2}:3/4:1\frac{1}{2}:3:1\frac{1}{2}$ consistent with the presence of syn,syn- and syn,anti isomers in an approximately statistical

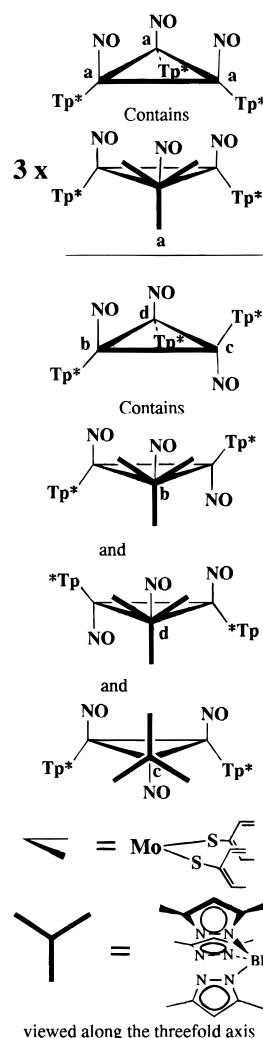


Figure 2. The effect of isomerism on the ^1H NMR signals of the tp* ligands in $[\text{Mo}(\text{NO})(\text{Tp}^*)(\text{SCH}_2)_2\text{C}_6\text{H}_4]_3$, complexes **5** and **10**.

ratio. The intensities of the signals due to the pyrazolyl methyl protons were obscured to some extent by overlap but were in accord with the proposed statistical isomer distribution.

The complexes **7–10** (Figure 1) were obtained from the reactions between 1,4-xylenedithiol and $[\text{Mo}(\text{NO})(\text{tp}^*)\text{I}_2]$ or $[\{\text{Mo}(\text{NO})(\text{tp}^*)\}_2\{1,4-(\text{SCH}_2)_2\text{C}_6\text{H}_4\}]$, **11**. Once again monometallomacrocycles, **7** and **8**, containing disulfide-linked xylenedithiol oligomers were isolated in addition to the expected cyclic oligomers **9** and **10** (Figure 1). However, in this case no thioether-linked macrocycle, comparable to **2**, could be detected. The infrared spectra of these compounds contained bands attributable to ν_{BH} at ca. 2550 cm^{-1} and ν_{NO} at ca. 1650 cm^{-1} in accord with the presence of the $\{\text{Mo}(\text{NO})(\text{tp}^*)\}$ moiety. The ^1H NMR spectra of **7** and **8** contained signals of relative areas 2:1 in the region δ 5.7–6.0 and 6:6:3:3 in the region 2.3–2.8 ppm, suggesting structures in which the tp* ligand is bisected by a plane of symmetry. The relative areas of the signals due to the tp* ligand protons and those of the aryl ligands in the spectra of **7** and **8** indicate that the respective tp*: $-\text{CH}_2\text{C}_6\text{H}_4-$ ratios are 1:2 and 1:3. In accord with this the LSIMS spectra were found to contain molecular ions at $m/z = 760$ (**7**) and 928 (**8**) leading to the formulations $[\text{Mo}(\text{NO})(\text{tp}^*)\{1,4-(\text{SCH}_2)_2\text{C}_6\text{H}_4\}_2]$, **7**, and $[\text{Mo}(\text{NO})(\text{tp}^*)\{1,4-(\text{SCH}_2)_2\text{C}_6\text{H}_4\}_3]$, **8**, which were confirmed by the single-crystal X-ray diffraction studies discussed below. These monometallomacrocycles were formed in slightly lower yields than their counterparts **1–3**

(21) (a) McQuillan, F. S.; Chen, H.; Hamor, T. A.; Jones, C. J.; Paxton, K. *Inorg. Chem.* **1997**, *36*, 4458–4464. (b) Jones, C. J.; McQuillan, F. S. Unpublished results.

(Table 1), and once again, the reaction involving $[\{\text{Mo}(\text{NO})(\text{tp}^*)\}_2\{1,4\text{-(SCH}_2)_2\text{C}_6\text{H}_4\}]$ produced lower yields of **7** and **8** than the reaction involving $[\text{Mo}(\text{NO})(\text{tp}^*)\text{I}_2]$.

In contrast to the reactions involving 1,3-xylenedithiol, where the cyclic dimer **4** was the major product, the reactions with 1,4-xylenedithiol afforded the cyclic trimer, **10**, as the major product with the cyclic dimer, **9**, being isolated in slightly lower yield. The syn,syn and syn,anti isomers of **10** could not be separated, but the syn and anti isomers of **9** were separated by repeated column chromatography. The two isomers **9a** and **9b** give molecular ions at $m/z = 1183$ in their LSIMS spectra in accord with their formulation as cyclic dimers. Although the ^1H NMR spectra of **9a** and **9b** differ, they do not define which is the syn and which the anti isomer, but on the grounds of solubility **9a** may be tentatively assigned the anti and **9b** the syn structures (vide supra). In both cases the pattern of signals attributable to protons in the tp^* ligand is in accord with the presence of a plane of symmetry bisecting the molecule and the relative areas of the signals due to the tp^* and xylyl protons are consistent with a $\text{tp}^*:\text{-(CH}_2)_2\text{C}_6\text{H}_4\text{-}$ ratio of 1:1. Dynamic behavior was again apparent in the ^1H NMR spectra of these compounds. The methylene proton signals of **9a** are not observed at room temperature but appear at elevated temperatures. In contrast, the spectrum of **9b** becomes very complex at elevated temperatures compared to the room-temperature spectrum. The activation energies for the dynamic processes appear to differ between the two isomers, but within the temperature range accessible, it was not possible to obtain meaningful activation energy values. The isomer distributions for the one- and two-step synthetic routes could be determined from the ^1H NMR spectrum of the crude product fraction **9** prior to separation of **9a** and **9b**. In both cases the red isomer, **9a**, was obtained in slightly lower yield (45%) than the brown isomer, **9b** (55%). However, this small difference in yield suggests that the reaction is essentially unselective.

The cyclic trimer, **10**, was obtained in rather higher yields (37–40%) than found for its counterpart **5**, but there was no significant difference in yield between the reactions involving $[\text{Mo}(\text{NO})(\text{tp}^*)\text{I}_2]$ and $[\{\text{Mo}(\text{NO})(\text{tp}^*)\}_2\{1,4\text{-(SCH}_2)_2\text{C}_6\text{H}_4\}]$ (Table 1). The LSIMS spectrum of **10** contained a molecular ion at $m/z = 1775$ in accord with its formulation as a cyclic trimer and contained no significant ion intensity attributable to the cyclic dimer at $m/z = 1183$. As with **5** this complex can exist as syn,syn or syn,anti isomers which could not be separated by column chromatography or fractional crystallization. The ^1H NMR spectrum of the tp^* protons in the isomer mixture was quite well resolved at room temperature and contained signals attributable to both isomers with some signal overlap. The relative intensities expected for the tp^* proton signals in a statistical mixture of the syn,syn and syn,anti isomers may be derived as described for **5**. The relative intensities observed for the pyrazolyl C^4 proton signals are $^{3/4}:1^{1/2}:1^{1/2}:^{3/4}:4^{1/2}$, consistent with the presence of syn,syn and syn,anti isomers in an approximately statistical ratio of 1:3.

In the presence of triethylamine, 1,2-xylenedithiol reacted with $[\text{Mo}(\text{NO})(\text{tp}^*)\text{I}_2]$ to give the chelate complex $[\text{Mo}(\text{NO})(\text{tp}^*)\{1,2\text{-(SCH}_2)_2\text{C}_6\text{H}_4\}]$, **12**, as the major product. Cyclic oligomers of formulas $[\{\text{Mo}(\text{NO})(\text{tp}^*)\}\{1,2\text{-(SCH}_2)_2\text{C}_6\text{H}_4\}]_n$ ($n = 2, 3$) or monometallomacrocycles of formulas $[\text{Mo}(\text{NO})(\text{tp}^*)\{1,2\text{-(SCH}_2)_2\text{C}_6\text{H}_4\}]_n$ ($n = 2, 3$) were not detected among the reaction products. However, the binuclear μ -oxo complex, $[\{\text{Mo}(\text{NO})(\text{tp}^*)\}_2\{\mu\text{-}1,2\text{-(SCH}_2)_2\text{C}_6\text{H}_4\}(\mu\text{-O})]$, was isolated in trace amounts and identified by LSIMS. The yield of **12** (55%) is comparable to those of the cyclic dimers formed in the

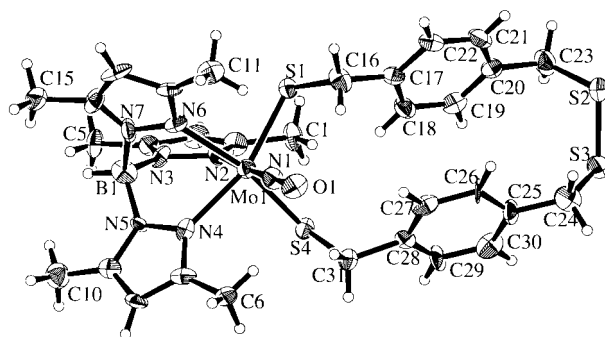


Figure 3. View of the complex **7**.

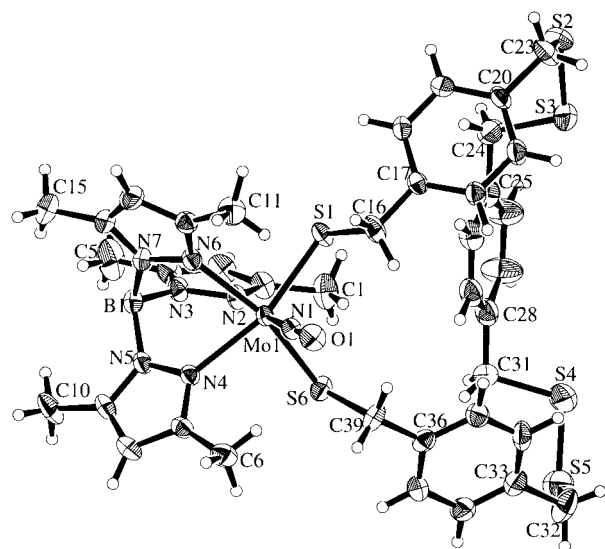


Figure 4. View of the complex **8**; view direction as for Figure 3.

reactions with 1,3- and 1,4-xylenedithiol. The infrared spectra of **12** contained bands at 2543 and 1650 cm^{-1} attributable to ν_{BH} and ν_{NO} , respectively. In the ^1H NMR spectrum, the relative intensities of the signals attributable to the protons of the tp^* ligand are in accord with the tp^* ligand being bisected by a plane of symmetry. The relative areas of the signals due to the tp^* ligand protons and those of the $\{1,2\text{-(CH}_2)_2\text{C}_6\text{H}_4\}$ moiety are consistent with their presence in a 1:1 ratio, and the LSIMS spectrum contained a molecular ion at $m/z = 592$ in accord with a monomeric formulation.

Structural Studies. Views of the complexes **7** and **8** are shown in Figures 3 and 4, which also illustrate the atomic numbering scheme used, and selected geometrical parameters are listed in Table 3. In both complexes the coordination geometry at the molybdenum atom is essentially octahedral, with maximum angular deviations from ideal octahedral of 17.7° (**7**) and 17.1° (**8**) for angle N(4)–Mo–S(1), mean deviation 6.9° in both structures. These deviations, however, show a consistent pattern, so that the mean deviation between corresponding angles at Mo in **7** and **8** is only 1.2°. Comparison with other octahedral $\{\text{Mo}(\text{NO})(\text{tp}^*)\}$ thiolato complexes, $[\text{Mo}(\text{NO})(\text{tp}^*)\{\text{S}(\text{CH}_2)_2\text{-CONH}(\text{CH}_2)_2\text{S}\}]$,²² $[\text{Mo}(\text{NO})(\text{tp}^*)\{\text{SCH}_2\text{CONHCH}_3\}_2]$,²³ and $[\text{Mo}(\text{NO})(\text{tp}^*)\{\text{S}(\text{CH}_2)_2\text{CONHCH}_3\}_2]$,²³ indicates that the mean deviations between corresponding angles at Mo are also quite small, in the range 0.7–1.4°. Common features are the smaller than 90° angles between the nitrogen atoms of the tp^* ligand

(22) Huang, J.; Ostrander, R. L.; Rheingold, A. L.; Walters, M. A. *Inorg. Chem.* **1995**, *34*, 1090–1093.

(23) Huang, J.; Ostrander, R. L.; Rheingold, A. L.; Leung, Y.; Walters, M. A. *J. Am. Chem. Soc.* **1994**, *116*, 6769–6776.

Table 3. Geometrical Parameters for **7** and **8**^a

	7	8
Bond Lengths (Å)		
Mo–N(1)	1.729(8)	1.758(4)
Mo–N(2)	2.256(9)	2.261(4)
Mo–N(4)	2.230(9)	2.233(4)
Mo–N(6)	2.237(8)	2.238(4)
Mo–S(1)	2.340(3)	2.339(2)
Mo–S*	2.365(3)	2.345(2)
N(1)–O(1)	1.223(11)	1.204(5)
S(1)–C(16)	1.813(11)	1.821(5)
S*–C*	1.814(11)	1.828(5)
Bond Angles (deg)		
N(1)–Mo–N(2)	177.4(4)	176.4(2)
N(1)–Mo–N(4)	94.6(4)	98.5(2)
N(1)–Mo–N(6)	97.5(4)	96.6(2)
N(1)–Mo–S(1)	94.5(3)	92.9(1)
N(1)–Mo–S*	92.6(3)	92.8(1)
N(2)–Mo–N(4)	87.6(3)	84.9(2)
N(2)–Mo–N(6)	84.4(3)	85.6(2)
N(2)–Mo–S(1)	83.7(2)	84.2(1)
N(2)–Mo–S*	85.9(2)	85.8(1)
N(4)–Mo–N(6)	76.0(3)	76.1(1)
N(4)–Mo–S(1)	162.3(2)	162.9(1)
N(4)–Mo–S*	92.1(2)	90.1(1)
N(6)–Mo–S(1)	87.9(2)	89.9(1)
N(6)–Mo–S*	164.9(2)	164.3(1)
S(1)–Mo–S*	102.6(1)	102.3(1)
Mo–N(1)–O(1)	175.5(8)	176.7(4)
Mo–S(1)–C(16)	110.1(5)	110.8(2)
Mo–S*–C*	113.4(4)	112.9(2)
Torsion Angles (deg)		
S*–Mo–S(1)–C(16)	–78.1(4)	–83.8(2)
Mo–S(1)–C(16)–C(17)	117.8(9)	170.3(3)
S(1)–C(16)–C(17)–C(18)	–39.7(15)	–133.2(5)
C(19)–C(20)–C(23)–S(2)	–107.5(12)	103.7(6)
C(20)–C(23)–S(2)–S(3)	81.3(11)	–44.7(5)
C(23)–S(2)–S(3)–C(24)	–100.8(6)	91.6(3)
S(2)–S(3)–C(24)–C(25)	97.9(11)	–167.1(4)
S(3)–C(24)–C(25)–C(26)	–120.9(12)	–84.6(7)
C(27)–C(28)–C(31)–S(4)		75.8(8)
C(28)–C(31)–S(4)–S(5)		167.1(5)
C(31)–S(4)–S(5)–C(32)		–94.4(4)
S(4)–S(5)–C(32)–C(33)		63.0(6)
S(5)–C(32)–C(33)–C(34)		–101.8(7)
C\$–C!–C*–S*	103.2(11)	111.7(6)
C!–C*–S*–Mo	–105.7(8)	–152.9(4)
C*–S*–Mo–S(1)	97.4(4)	84.1(2)

^a S* is S(4) in **7** and S(6) in **8**; C* is C(31) in **7** and C(39) in **8**; C\$ is C(27) in **7** and C(35) in **8**; C! is C(28) in **7** and C(36) in **8**.

and the greater than 90° angles between the nitrosyl nitrogen atom and the other two ligands. A further common feature is that the trans angle involving the nitrosyl nitrogen atom is significantly closer to 180° (range 175.8–178.4°) than the other two trans angles (range 160.4–164.9°). The same pattern of angular variation is observed in all known octahedral complexes based on the {Mo(NO)(tp*)} moiety, such as, for example, [Mo(NO)(tp*)(2-NHC₃H₄N)₂].²⁴ When compared with our structures **7** and **8**, mean deviations between corresponding coordination angles are 1.6 and 1.8°, respectively.

The bonds to the pyrazolyl ring nitrogen atoms, 2.230–2.261 Å, are similar in length to those measured in the complexes cited^{22–24} above, 2.229–2.249,²² 2.210–2.256,²³ and 2.210–2.242 Å.²⁴ In every case the bond trans to the nitrosyl group is the longest, being in the range 2.241–2.261 Å, whereas the other two bonds in these six structures are 2.210–2.238 Å; presumably this effect is due to the trans bond-lengthening

influence of the strongly π accepting nitrosyl ligand. The short Mo–N(nitrosyl) bond lengths in **7** and **8** are also in agreement with previous results and are indicative of a strong bonding interaction. The Mo–S lengths, mean 2.352 (**7**) and 2.342 Å (**8**), and Mo–S–C angles, mean 111.8° (**7**) and 111.9° (**8**), are similar to those measured^{22,23} in analogous thiolato complexes, mean Mo–S, 2.346 Å, mean Mo–S–C angle, 112.0°. In contrast analogous oxo complexes^{25,26} have much larger angles at oxygen, 128.8–133.4°, and relatively shorter Mo–O bonds, 1.900–1.910 Å attributed^{25,26} to $p\pi$ – $d\pi$ donation from oxygen to molybdenum. In the thiolato complexes there is, therefore, less evidence of $p\pi(S)$ – $d\pi(Mo)$ orbital overlap, although the near-coplanarity of the C–S–Mo–NO moieties, torsion angles N(1)–Mo–S–C 15.6(5) and 2.2(5)° in **7** and 9.7(3) and –9.4(3)° in **8**, would be favorable for such overlap to occur. There is also some shortening of the Mo–S bonds when compared with the mean length of 2.401 Å given by Orpen et al.²⁷ for such bonds in Mo–S–C(sp³) moieties.

In the oligomeric disulfide-linked 1,4-xylene ring systems, the dibenzyl disulfide fragments have bond lengths in good agreement with those found²⁸ in the crystal structure of dibenzyl disulfide itself. Thus S–S bonds, 2.020(5) Å in **7** and 2.018(3), 2.012(3) Å in **8**, compare with 2.015 Å in dibenzyl disulfide. In **7**, the overall shape of the central ring is rather irregular (see Figure 3 and torsion angles in Table 3). The two phenyl rings are nearly parallel, dihedral angle 8.7(7)°. Close cross-ring distances between these rings occur, C(17)···C(27) 3.539 Å, C(18)···C(26) 3.461 Å, C(18)···C(27) 3.272 Å, C(19)···C(26) 3.506 Å. In **8** the ring system adopts a more symmetrical form. Inspection of the endocyclic torsion angles shows that, to a first approximation, it possesses mirror (*C_s*) symmetry, the pseudoplane passing through the molybdenum atom and the centers of the C(26)–C(27) and C(29)–C(30) bonds (see Figure 5). The boron atom, the nitrosyl ligand, and the pyrazolyl ring comprising atoms N(2), N(3), and C(2)–C(4), trans to the NO ligand, also lie close to this plane. Relative to its mean plane, the ring [taken to be the 19 atoms Mo, S(1), C(16), C(17), C(20), ..., S(6), i.e., including only those atoms of the phenyl rings bonded to SCH₂ residues] shows a systematic ruffling effect, with maximum deviations below the ring plane at molybdenum (–1.37 Å) and at the C(25)···C(28) moiety (–1.42 Å), at diametrically opposed ends of the ring. Intermediate between these negative deviations, deviations of approximately the same amount above the ring plane occur at C(23) (1.47 Å) and at C(32) (1.53 Å). Cross-ring distances of interest include C(1)···C(29) 3.442 Å, C(1)···C(30) 3.757 Å, C(18)···C(30) 3.740 Å, and C(29)···C(35) 3.795 Å.

Electrochemical Studies. The cyclic voltammograms of the new complexes, measured in CH₂Cl₂ solution, all contain well-formed reduction waves associated with the presence of the {Mo(NO)}³⁺ center, and the data obtained are summarized in Table 4. The waves were, for the most part, chemically reversible on the cyclic voltammetry time scale in that the cathodic to anodic current ratio was usually close to 1. However, the waves generally showed poor electrochemical reversibility with anodic to cathodic peak potential separations

(24) AlObaidi, N.; Hamor, T. A.; Jones, C. J.; McCleverty, J. A.; Paxton, K. *J. Chem. Soc., Dalton Trans.* **1987**, 1063–1069.

(25) McCleverty, J. A.; Rae, A. E.; Wolochowicz, I.; Bailey, N. A.; Smith, J. M. *A. J. Chem. Soc., Dalton Trans.* **1982**, 951–965.

(26) AlObaidi, N. J.; Salam, S. S.; Beer, P. D.; Bush, C. D.; Hamor, T. A.; McQuillan, F. S.; Jones, C. J.; McCleverty, J. A. *Inorg. Chem.* **1992**, *31*, 263–267.

(27) Orpen, A. G.; Brammer, L.; Allen, F. H.; Kennard, O.; Watson, D. G.; Taylor, R. In *International Tables for Crystallography*; Wilson, A. J. C., Ed.; Kluwer Academic Publishers: Dordrecht, 1995; Vol. C.

(28) van Dijk, B.; Visser, G. J. *Acta Crystallogr., Sect. B* **1971**, *27*, 846.

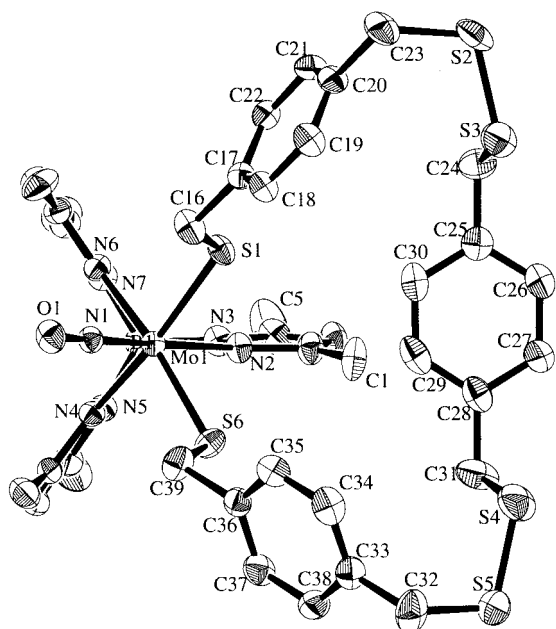


Figure 5. View of the complex **8** along the Mo...B axis illustrating the pseudo mirror symmetry. Hydrogen atoms have been omitted.

Table 4. Electrochemical Data and Nitrosyl Stretching Frequencies

compd	E_f (V) ^a	ΔE_p (mV) ^b	i_{pa}/i_{pc} ^c	ΔE_p (Fc/Fc ⁺) (mV) ^d	$\nu_{\max}(\text{NO})$ (cm ⁻¹) ^e
1	-1.388	240	1.00	76	1653
2	-1.417	273	0.86	85	1654
3	-1.400	415	0.81	76	1644
4a	-1.421 ^f	183	0.60	85	1655
4b	-1.389 ^f	493	0.97	83	1653
5	-1.397 ^g	149	0.58	94	1654
6	-0.933	122	0.95	75	1674
7	-1.375	181	0.98	77	1647
8	-1.369	211	1.00	94	1652
9a	-1.486 ^f	288	0.96	70	1656
9b	-1.422 ^f	246	1.06	91	1654
10	-1.374 ^g	117	0.89	95	1652
11	-0.945	242	0.98	97	1676
12	-1.269	100	0.94	89	1628

^a Formal electrode potential of the *complex* from cyclic voltammograms obtained under an inert atmosphere at a Pt bead electrode from ca. 10^{-3} mol dm⁻³ solutions in dry CH₂Cl₂ containing 0.2 mol dm⁻³ [Bu₄N][BF₄] as the supporting electrolyte. Potentials were measured versus a ferrocene added as an internal standard. Against a saturated calomel reference electrode E_f for Fc/Fc⁺ fell in the range 0.547–0.562 V. ^b Separation between the potentials corresponding to the peak cathodic and anodic currents. ^c Ratio of the anodic and cathodic peak currents. ^d Separation between the potentials corresponding to the peak cathodic and anodic currents for the ferrocene/ferrocenium couple at a diffusion current similar to that of the *complex*. ^e Obtained from KBr disks. ^f Wave presumed to involve two unresolved one-electron processes associated with two weakly interacting or non-interacting metal centers. ^g Wave presumed to involve three unresolved one-electron processes associated with three weakly interacting or non-interacting metal centers.

ranging from 100 to 493 mV compared to values of less than 100 mV for the ferrocene standard. In the case of the simple mononuclear chelate complex **12** a single reversible reduction wave was observed at -1.269 V (vs Fc/Fc⁺). The mononuclear complexes containing dithiol ligand oligomers reduced at more negative potentials ranging from -1.369 V for **8** to -1.417 V for **2**. This shift in reduction potential may be due to increased flexibility in the larger chelate rings allowing improved overlap between the sulfur filled p and molybdenum unoccupied d_{xy}

orbitals which are involved in the LUMO of the complex. This would lead to increased electron density on the metal center and a more negative reduction potential. Such effects on the reduction potentials of complexes containing the {Mo(tp*)(NO)-(S)₂} moiety have been observed previously.²⁹ Photoelectron spectroscopy studies of the related Mo(V) chelate complexes [Mo(tp*)(=O){O(CH₂)_nO}] ($n = 2-4$) indicate that the energy of the HOMO, which in this system is the MO which involves d_{xy}, is also sensitive to chelate ring size, increasing in energy with increasing n .³⁰ The low value of ν_{NO} for **12** (1628 cm⁻¹) compared to those of the other mononuclear chelates (1644–1654 cm⁻¹) would seem to be at odds with the reduction potential data in suggesting that **12** has the highest electron density at the metal ion. However, the LUMO involved in the reduction reactions involves the metal d_{xy} orbital whereas the metal orbitals associated with π -bonding between Mo and NO would be d_{xz} and d_{yz}, so that the simple correlation between reduction potential and ν_{NO} found previously³¹ for nonchelated complexes may not be retained in systems which are sterically constrained by chelate formation.

The binuclear complexes **4a**, **4b**, **9a**, and **9b** each show a single reduction wave in the region -1.369 to -1.486 V. As two equivalent redox centers are present in these complexes, these waves comprise two one-electron-reduction processes. Where substantial interactions between the metal centers are present, two one-electron-reduction waves will be expected.^{13d,21a,32} However, if the metal centers interact only weakly, or not at all, as appears to be the case here, cyclic voltammetry could not be expected to resolve the two processes. This behavior has been found previously for related acyclic binuclear complexes in which the ligands linking the metal centers contain methylene groups.³³ Most surprising are the observed differences in electrochemical behavior between the members of each pair of isomers, **4a** and **4b** and **9a** and **9b**. The complex **4a** reduces at -1.421 V, a potential 32 mV more negative than that of -1.389 V found for **4b**. Furthermore **4a** shows chemical irreversibility ($i_{pa}/i_{pc} = 0.60$) and a ΔE_p value of 183 mV in contrast to the behavior of **4b**, which shows a chemically reversible ($i_{pa}/i_{pc} = 0.97$) reduction but has a much larger ΔE_p value (493 mV). In the case of **9a** and **9b** similar i_{pa}/i_{pc} and ΔE_p values are found for each isomer but the E_f values are again different, in this case by 64 mV. This is the first time that clear differences in the electrochemical properties of isomerically related complexes have been observed. Although the differences in E_f are small, they nonetheless lie outside the probable maximum measurement error of 10 mV assuming errors of ± 5 mV for each potential measured against the internal ferrocene standard. The reasons for these differences in behavior presumably lie in the conformational demands of the metallomacrocyclic ring. These may impose different (O)N–Mo–S–C(H₂) torsion angles in the different isomers and, by affecting the orientation of the filled sulfur p orbitals with Mo d_{xy}, will affect the redox properties of the complex.^{29,30} Any increased ring strain could also affect chemical reversibility. If, as seems likely,²⁰ reduction

(29) (a) Obaidi, N. A.; Jones, C. J.; McCleverty, J. A. *Polyhedron* **1989**, *8*, 1033–1037. (b) Ashby, M. T.; Enemark, J. H. *J. Am. Chem. Soc.* **1986**, *108*, 730–733.

(30) Chang, C. S.; Rai-Chaudhuri, A.; Lichtenbutget, D. L.; Enemark, J. H. *Polyhedron* **1990**, *9*, 1965–1973.

(31) Obaidi, N. A.; Chaudhuri, M.; Clague, D.; Jones, C. J.; Pearson, J. C.; McCleverty, J. A.; Salam, S. S. *J. Chem. Soc., Dalton Trans.* **1987**, 1733–1736.

(32) Charsley, S. M.; Jones, C. J.; McCleverty, J. A.; Neaves, B. D.; Reynolds, S. J. *J. Chem. Soc., Dalton Trans.* **1988**, 301–307.

(33) Charsley, S. M.; Jones, C. J.; McCleverty, J. A.; Neaves, B. D.; Reynolds, S. J. *J. Chem. Soc., Dalton Trans.* **1988**, 301–307.

Table 5. Electronic Spectra

compd	$\lambda_{\text{max}}/\text{nm}$ ($\epsilon/\text{dm}^3 \text{ mol}^{-1} \text{ cm}^{-1}$) ^a			
1	365 (6800)	478 (4600)		
2	365 (8700)	467 (6100)		
3	338 (7700)	476 (5400)		
4a	368 (17 000)	468 (13 000)	589 (4700)	
4b	366 (14 400)	468 (11 300)	589 (3800)	
5	368 (13 500)	468 (12 700)	589 (3100)	
6	290 (700)	395 (1400)	493 (900)	
7	363 (3200)	483 (2700)		
8	368 (1600)	478 (1200)		
9a	365 (8700)	467 (6700)	580 (2400)	
9b	358 (12 400)	475 (8400)	590 (3200)	
10	365 (8000)	475 (10 600)	590 (3500)	
11	395 (10 200)	495 (6700)		
12	352 (5200)	418 (12 400)	490sh (4200)	768 (1900)

^a Recorded from ca. 10^{-5} mol dm⁻³ solutions of the complex in dry CH₂Cl₂.

labilizes the metal center, then ring opening might occur more readily in strained rings, leading to an irreversible reduction process, although there is no direct evidence that this is the source of the chemical irreversibility.

Electronic Spectra

The electronic spectra of the new complexes were recorded from solutions in CH₂Cl₂. All contained an intense absorption at ca. 230 nm which is also observed in the spectrum of Ktp* and may be attributed to a $\pi-\pi^*$ transition associated with the tp* ligand.^{20b} The other bands observed in the spectra are summarized in Table 5 and are too intense to be attributed to d-d transitions. In all of the spectra of the cyclic compounds, bands are present at ca. 365 and ca. 470 nm which may result from ligand to metal charge transfer processes arising from the electron acceptor properties of the metal center. In addition the spectra of the cyclic oligomers **4a**, **4b**, **5a**, **5b**, **9**, and **10** contain a less intense, lower energy band at ca. 585 nm which appears to be unique to the oligomeric metallomacrocycles. The spectrum of the chelate complex, **12**, also contains a lower energy band but in this case at the longer wavelength of 768 nm. These differences in spectroscopic properties may reflect the differing structural constraints applied to the {Mo(NO)(tp*)} center by its inclusion in cyclic structures of differing size. Such effects have also been observed previously in the photoelectron spectra of the alkoxide complexes [Mo(=O)(tp*)(OR)₂] (R = Me, Et, ⁿPr) and their chelated counterparts [Mo(=O)(tp*)(E-E)] {E-E = O(CH₂)_nO, $n = 2-4$ }.³⁰

Conclusion

An unexpected feature of the reactions between [Mo(tp*)(NO)I₂] and 1,3- or 1,4-xylenedithiol is the formation of significant yields of the monometallic products **1**, **2**, **3**, **7**, and **8** in which ligand oligomerization has occurred through disulfide or thioether bond formation. Unsurprisingly, corresponding compounds have not been observed with related oxygen donor ligands. These would involve peroxide formation, and [Mo(tp*)(NO)I₂] would not be expected to effect such a reaction nor would peroxide-containing products, if formed, be expected to be stable to chromatography under the conditions used.

The distribution of products obtained from these reactions demonstrates the sensitivity of the metallomacrocyclic formation process to the orientation of donor substituents on the aryl ring. As might be expected, the reaction with 1,2-(HSCH₂)₂C₆H₄ affords the 1:1 chelate complex as the only significant product. In the cases of 1,3- and 1,4-(HSCH₂)₂C₆H₄ chelation is not possible and cyclic dimers and trimers are obtained. Although the cyclic dimers might be favored on purely statistical grounds, bringing together four rather than six components, the reaction involving 1,4-(HSCH₂)₂C₆H₄ produces higher yields of the cyclic trimer than of the dimer. This finding presumably reflects the differing structural constraints imposed by the pattern of substitution at the aryl ring. The 1,3-substitution pattern appears sufficiently well suited to the cyclic dimer structure that this product predominates over the cyclic trimer to the extent of about 5:1. However, the 1,4-substitution pattern leads to the formation of slightly more trimer than dimer, contrary to statistical expectations but in accord with an increased angle between the C(aryl)-C(methylene) bonds in the bifunctional ligand. It is notable that the reactions between 1,*x*-(HSCH₂)₂C₆H₄ ($x = 3, 4$) and [{Mo(NO)(tp*)}₂{1,*x*-(SCH₂)₂C₆H₄}] also afford some cyclic trimer. This suggests that, during the reaction, some ligand exchange must be occurring to create monometallic fragments, although the cyclic dimers themselves seem to be kinetically stable once formed. Although there are small differences between the yields of the syn and anti isomers of the cyclic dimers, the selectivity of these reactions is poor. The reaction of preformed [{Mo(NO)(tp*)}₂{1,*x*-(SCH₂)₂C₆H₄}] with further xylenedithiol offers a more structured approach to the synthesis of the cyclic dimers and trimers. However, the relatively poor yields encountered in the syntheses of the bimetallic complexes **6** and **11** render this approach less efficient than the direct one-step synthesis from [Mo(tp*)(NO)I₂].

The first definitive evidence that the electrochemical properties of metallomacrocycles of this type can be affected by isomer structure has been obtained. Although the effects are modest, they are outside the expected measurement errors and have been observed in two different isomer pairs, in **4a** and **4b** and in **9a** and **9b**. These results indicate that the structural constraints imposed on a transition metal ion, by its incorporation within a macrocyclic ring, may affect its electronic structure and lead to properties which differ from those of a corresponding acyclic complex.

Acknowledgment. We are grateful to Mr. P. R. Ashton for mass spectrometric measurements. We thank the EPSRC (GR/J87572), the Leverhulme Trust, and the University of Birmingham for supporting this work (F.S.McQ. and H.A.H.) and the EPSRC and the University of Birmingham for funds to purchase the R-Axis II diffractometer. We also thank the British Council for a Sino-British Friendship Scholarship to H.C.

Supporting Information Available: Listings of positional parameters, thermal parameters, distances, and angles (12 pages). Ordering information is given on any current masthead page.

IC971357F